EXPERIMENTAL STUDY OF ABLATION AND ENERGY TRANSPORT IN KrF LASER-PLASMA INTERACTION§

P. D. GUPTA†, A. A. OFFENBERGER*, R. FEDOSEJEVS*, R. POPIL* and Y. Y. TSUI*
Laser Division, Bhabha Atomic Research Centre, Bombay 400 085, India.
**Department of Electrical Engineering, University of Alberta, Edmonton, Alberta T6G 2G7, Canada.*

ABSTRACT

Results of an experimental study of ablation and energy transport in KrF laser-plasma interaction in moderate and high-Z targets are presented. Planar targets of plastic, aluminium and gold were irradiated in the intensity range of 10^{11}–2×10^{13} W/cm^2 by focussing KrF laser pulses from a high power laser system employing Raman or Brillouin pulse compression techniques. Measurements of electron temperature, backreflectivity, hydrodynamics, heat penetration and soft X-ray emission were performed on bare and coated targets. For moderate-Z targets the results are in good agreement with the prediction of a plasma ablation model based on inverse bremsstrahlung dominated absorption and uninhibited electron thermal transport. In contrast, for high-Z gold target, quite different ablation and heat penetration characteristics are observed. These results are discussed in terms of occurrence of a significant inward radiation energy transport and radiation loss from high-Z plasma.

INTRODUCTION

RECENTLY there has been a great emphasis on using high power lasers operating at short wavelengths for laser-induced fusion research. This has resulted from several advantages viz increased thermal absorption, reduced generation of hot electrons and target preheat, higher ablation rate and ablation pressure observed in short wavelength laser-plasma interaction experiments[1,2]. Use of KrF lasers operating at 0.25 μm as a potential fusion driver is particularly attractive in this regard on account of their higher overall efficiency. Study of laser plasma interaction using KrF laser radiation has thus become quite important. In this paper, we report a detailed experimental study of ablation and energy transport in KrF laser interaction with plasma produced from moderate and high-Z targets in the laser intensity range of 10^{11}–2×10^{13} W/cm^2.

KrF LASER SYSTEM

A high power KrF laser system employing beam multiplexing and stimulated Raman or Brillouin scattering to provide peak powers in excess of 1 GW has been built to conduct laser-plasma studies at 0.25 μm wavelength[3]. The system consists of three major components viz (i) front end comprised of KrF discharge lasers, (ii) electron beam pump amplifier, and (iii) hybrid optical compressor. The front end is a multimodule system having a narrow linewidth oscillator followed by an injection-locked slave oscillator and two discharge module amplifiers[4]. Output of the front end is used to generate and amplify a short duration stokes pulse by Raman or Brillouin backward scattering in high pressure gas cells. Electron beam pump amplifier is a dual beam machine, both arms having a 5-stage Marx bank system and a

---

§Work performed at the Department of Electrical Engineering, University of Alberta.

† For correspondence.

water blumlein. The output of the e-beam amplifier is extracted in a 3-beam, 3-pass multiplexing arrangement and these 3 beams are used to amplify the short duration Stokes pulse generated in the initial stages of the system. Initially, the pulse compression was done using Raman backward scattering in high pressure methane gas[5]. In this scheme, the system gave an optical output at 0.268 μm with maximum energy of 2.2 J in a pulse of typically 2 nsec duration. These Raman pulses had a temporal modulation on a time scale of 200 to 400 psec with a depth of $\leqslant 50\%$. Subsequently pulse compression was done using stimulated Brillouin backscattering in high pressure SF_6 gas[6]. In this system, the optical output was obtained at 0.248 μm with peak energy of 3 J in a pulse of 1.5 to 2 nsec FWHM with little modulation.

The laser beam was focussed onto planar targets in a vacuum chamber using a 70 cm focal length quartz lens. The focal spot intensity distribution was monitored using an equivalent focal plane imaging system coupled to a video digitizer system. For the Raman compressed pulse, the average values for the best focus condition were such that the 50% and 90% energy contours had areas corresponding to equivalent diameters of 34 μm and 74 μm respectively. The focussed intensity ranged from 10^{11}–2×10^{13} W/cm^2 and was varied by changing the laser output energy or by moving the lens towards the target by 2 mm and 4 mm distances. The equivalent 90% energy containing diameters for the latter conditions were 170 μm and 340 μm respectively. For the Brillouin-compressed pulse, the 70% energy contour for best focus had an area corresponding to an equivalent diameter of 70 μm.

DIAGNOSTICS

Several diagnostics were used to study the laser-plasma interaction. Arrays of plasma calorimeters and Faraday cups were used to map the angular distribution of energy and ion velocity distribution in the expanding plasma. These ion diagnostics were used to determine the mass ablation rate and the ablation pressure. X-ray intensity measurements (keV) were performed by using cross-calibrated scintillator photomultiplier detectors and p-i-n diode for electron temperature measurements. Sub-keV X-ray emission was detected using biplanar X-ray diodes for estimation of X-ray conversion efficiency. The temporal history of the X-ray emission for energies above 1 keV was observed by an X-ray streak camera and was used to infer ablation rate from burn-through time in multilayered targets. Heat penetration in high-Z targets was measured with a luminosity time of flight spectrometer (LTOFS). A 0.58 m Ebert grating monochromator was used in conjunction with an optical multichannel analyser to spectrally resolve the backscattered laser light. Further, backscatter and specular reflectivity levels were measured using a fast response (< 0.5 nsec) vacuum photodiode and energy calorimeter. A UV streak camera was employed to temporally resolve the incident laser pulse and the evolution of backscattered light. Background pressure in the target chamber during all these measurements was maintained at approximately 10^{-5} torr.

EXPERIMENTAL RESULTS AND DISCUSSION

A number of experimental investigations were performed in plasmas produced from bare targets of plastic, aluminium, gold and gold-coated plastic targets with different gold overlayer thicknesses. Some important experimental results and their implications are briefly discussed. More details and discussion of the experimental results are contained in the given references.

a) *Electron temperature measurements*

Electron temperature measurements were performed using the foil transmission technique. The electron temperature was estimated by fitting the experimentally observed relative X-ray intensities transmitted through different foils with those calculated using either a collisional-radiative model or a corona model.

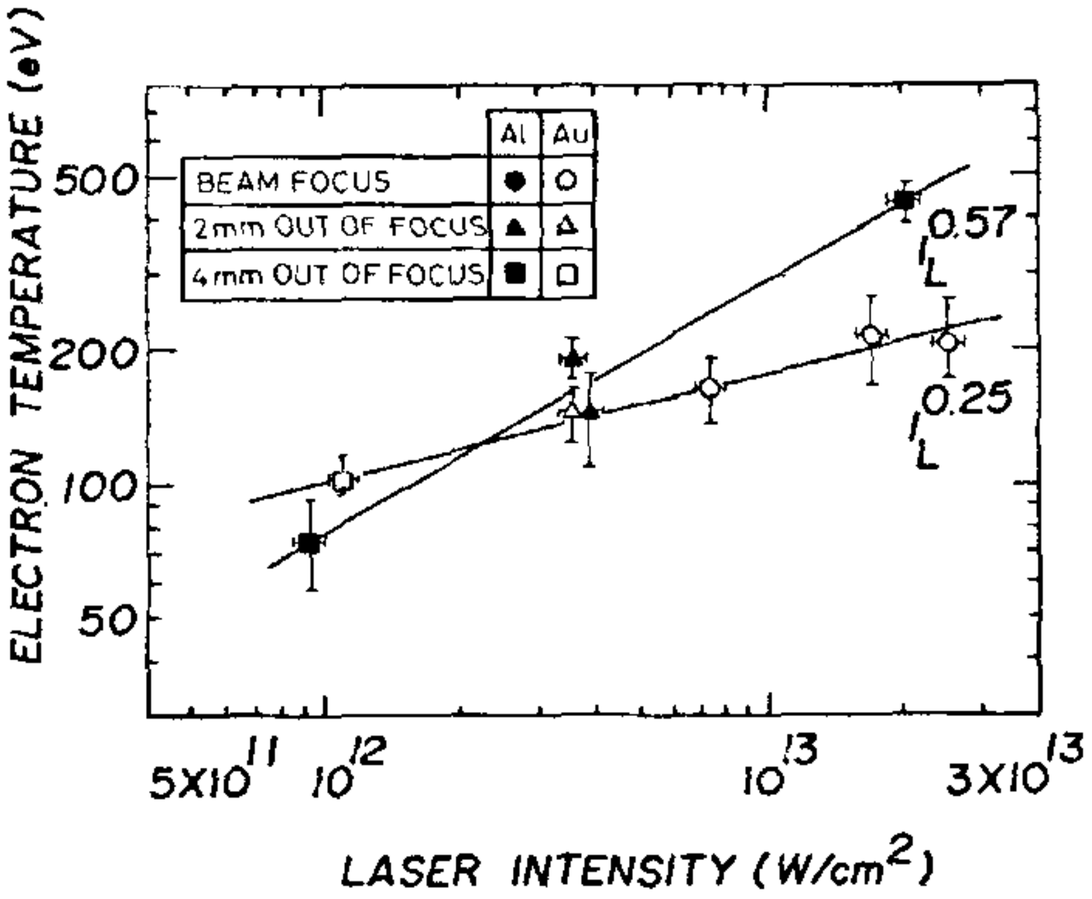

Figure 1. Dependence of the experimentally measured temperature on the laser intensity for aluminium and gold plasmas.

Sufficiently thick foils were used for high energy X-ray transmission to minimize complications due to line radiation. The results of these measurements for aluminium[7] and gold[8] plasmas at different laser intensities for best focus, 2 mm out of focus and 4 mm out of focus irradiation conditions are shown in figure 1. Comparison of measured temperatures and the scaling of temperature with laser intensity with those expected from a self-regulating model[9] based on inverse bremsstrahlung dominated absorption and uninhibited electron thermal transport showed good agreement for the aluminium plasma. Further X-ray intensity for the energy range 10 keV $\leqslant h\nu \leqslant$ 15 keV was smaller than 3×10^{-5} (detector limited) times the total X-ray intensity above 1 keV. Such a small energy content of 10 keV X-rays indicates a negligible level of hot electron generation at the present intensities.

In contrast to the above, the temperature scaling in the gold plasma is observed to be $T_e \propto I_L^{0.25}$ (figure 1) which is much slower than that for the self-regulating model ($T_e \propto I_L^{0.44\text{-}0.50}$). The measured temperatures are also considerably smaller than the predicted values from the model; e.g. at $I_L = 1.6\times10^{13}$ W/cm^2 the measured temperature is $T_e = 220\pm50$ eV in comparison to $T_e = 520$ eV expected from the model. This behaviour is thought to be due to radiation energy loss from the plasma and radiation-induced energy transport in the high-Z plasma[8].

b) *Specular reflectivity and stimulated Brillouin backscatter*

Characteristics of specular reflection and stimulated Brillouin backscatter (SBS) were studied[10] up to intensities of 10^{14} W/cm^2. Relatively higher laser intensities were achieved by using a short focal length lens (FL = 20 cm). Both the time resolved and the time integrated reflectivities were measured at three different angles of incidence $\theta = 0°$, 22.5° and 45°. The spectra of specularly reflected light and SBS were recorded with an overall spectral resolution of 0.34 Å. For most of these measurements, the laser was operated in the Brillouin-compressed mode. The laser output had a prepulse energy of 10–40 mJ commencing ~ 10 nsec prior to the main pulse, thus preforming a colder plasma of a scale length of ~ 80 μm.

For normal incidence, the plasma back-reflectivity was $\leqslant$ 1% and did not show much variation with laser intensity as the target was moved out of best focus position. The constancy of back-reflectivity even when the laser intensity is changed by more than two orders of magnitude indicates that the back-reflectivity is dominated by specular reflection from the plasma density gradient.

For non-normal incidence, the specular reflection and SBS are separated. Dependence of these two reflectivities on intensity was measured by moving the target away from the best focus position. Results of these measurements for $\theta = 45°$ for incident laser powers of 0.3 GW and 0.9 GW are shown in figure 2. The target position marked 0 corresponds to the best focus position. For the lower power, the specular reflectivity is ~ 4% compared to a value of ~ 0.1% for the SBS, and does not show much variation with target position. On the other hand, for the higher power, both specular and SBS reflectivities show a strong dependence on the target position. Whereas SBS reflectivity shows a peak value of 1.8% for

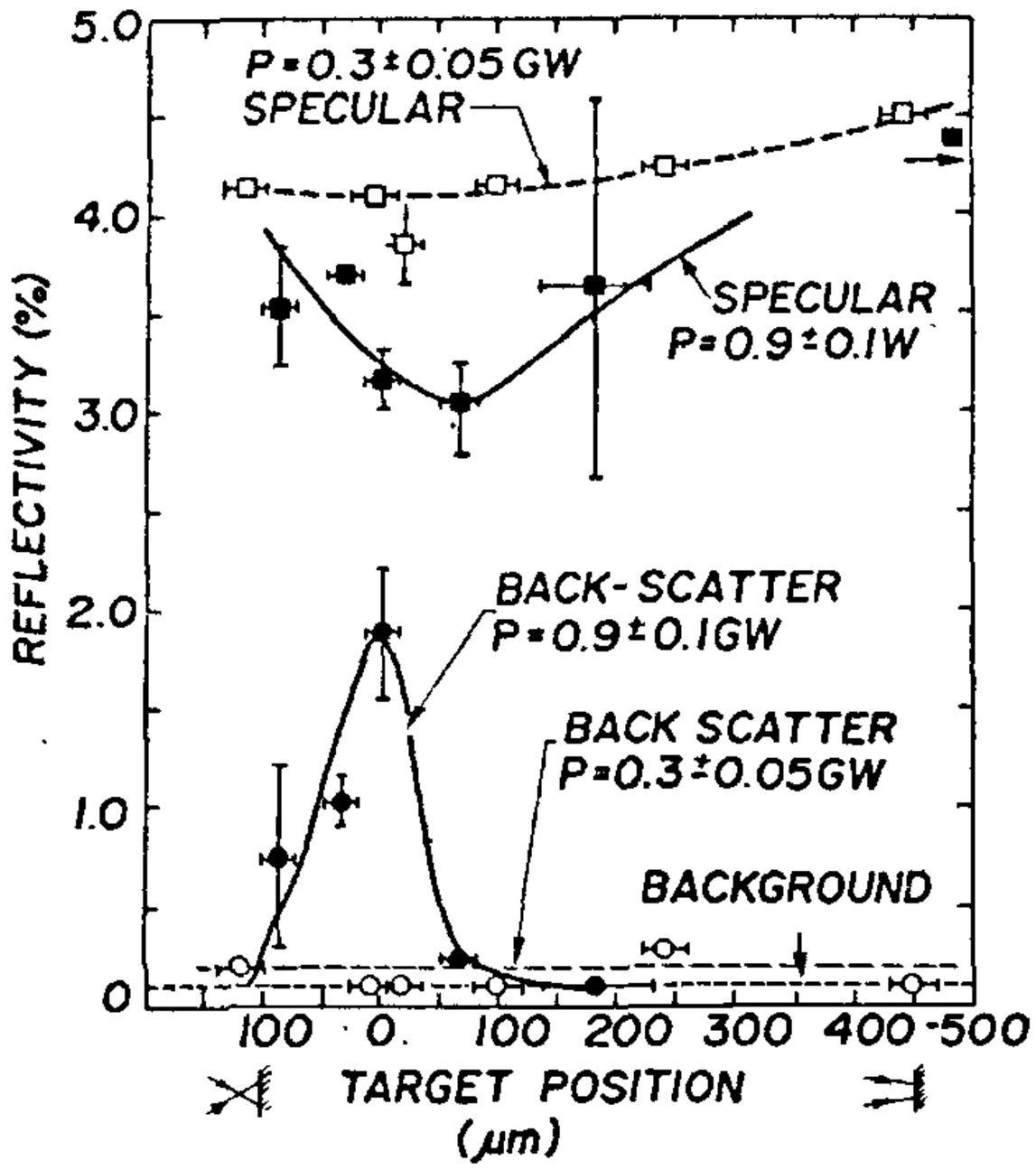

Figure 2. Dependence of backscatter and specular reflectivity on target position for an angle of incidence of 45°.

the best focus position, the specular reflectivity is higher for target positions away from the best focus.

The observed levels of SBS are consistent with the calculated SBS convection gain for the parameters of the experiment. The smaller levels of backreflectivity are in overall agreement with the high degree of laser energy absorption in the plasma expected for inverse bremsstrahlung dominated absorption in the underdense region of the plasma. This is supported from measurements of scattered light using an Ulbricht sphere showing that $97 \pm 2\%$ of the incident laser energy was absorbed for laser intensities up to $\sim 10^{13}$ W/cm^2.

c) *Mass ablation rate and ablation pressure*

The mass ablation rate and ablation pressure were measured for aluminium plasma using two different methods based on plasma expansion characteristics and X-ray burn-through of multilayered targets. Determination of mass ablation rate and ablation pressure from plasma expansion measurements is based on an estimation of the total ablated mass (M) and the ablation momentum ($p_\perp$) in the direction of target normal[11]. These quantities were determined from the experimental data of angular distributions of asymptotic ion expansion velocity using Faraday cups and of plasma energy using differential calorimeters. In the other method, temporal modulations of the X-ray emission from multilayered target were observed to determine the burn-through time of a given layer thickness using a soft X-ray streak camera.

The ion expansion characteristics of aluminium plasma was studied in detail for different laser intensities and irradiation conditions. It was observed that for the high intensity range of 5×10^{11}–10^{13} W/cm^2 for best focus and 2 mm out of focus irradiation, the ion current signals showed a two-peak behaviour. From the analysis of velocity scaling, angular distribution, velocity distribution and energy partition in two components, this behaviour is attributed to the occurrence of lateral heat conduction in the plasma[12]. This effect becomes important for small focal spot irradiation conditions where the thermal diffusion length exceeds the focal spot dimensions. The ions in the first peak correspond to the initial hot plasma, while those in the second peak correspond to the 3-D flow occurring over an effectively larger area heated by lateral thermal conduction.

In order to assess the influence of the lateral energy spread across the focal spot in the estimation of M and $p_\perp$, two different procedures of analysis were used. Details of these procedures are given in Ref. 11. The experimental scaling laws for mass ablation rate $\dot{m}$ and ablation pressure P_a were determined to be

$$\dot{m} = (1.5 \pm 0.1) \times 10^5 \, [I_L/10^{13} \, (\mathrm{W/cm^2})]^{0.42 \pm 0.02} \, \mathrm{g/cm^2\text{–}S}$$

and

$$p_a = (5.5 \pm 0.3) [I_L/10^{13} \, (\mathrm{W/cm^2})]^{0.81 \pm 0.02} \, M \text{ bar.}$$

These results are reasonably in good agreement with the theoretical values expected from the self-regulating model.

Mass ablation rate was also determined from the X-ray burn-through measurements in multilayered targets. The targets consisted of low-Z layer sandwiched between thin layers of high-Z material which serve as marker layers to measure ablation burn-through time of the low-Z layer. Ablation rate determined in this fashion[10] for the multilayered aluminium target showed somewhat higher values compared to the model results and those derived from the ion data. This is explained from the fact that X-ray burn-through measurements provide peak ablation rates corresponding to the maximum intensity in the focal spot.

d) *Energy transport measurements*

Energy transport in high-Z plasma was studied from the burn-through measurements of gold-coated plastic (CH) targets. Ablation burn-through of the gold layer was observed using a LTOFS[13] by detecting the onset of emission of CVI 3434 Å line in the plasma ablated from the CH target. Onset of CVI line emission corresponds to the arrival of the ~ 100 eV isotherm in the plastic substrate. These measurements are described in detail elsewhere[14].

Ablation burn-through was also observed from Faraday cups by comparing ion current signals for different targets. Although charge collectors do not distinguish between different ion species, the expansion velocity and the ion current are substantially different for gold and plastic plasmas. For example, a CH target irradiated at 1.5×10^{12} W/cm^2 ($T_e \sim 100$ eV), the velocity corresponding to the peak of ion current for CH plasma observed at $\theta = 15°$ was 2.1×10^7 cm/sec in comparison to that of 9×10^6 cm/sec for the thick gold target. The peak ion current for CH plasma was ~ 40 times larger than that for gold. Thus when a gold-coated plastic target is irradiated, appearance of a large current for $v \gtrsim 2.1 \times 10^7$ cm/sec would indicate penetration of the hot plasma ablation front into the plastic. A burn-through laser intensity of 4.7×10^{12} W/cm^2 was determined for 0.15 μm gold-coated target in this manner.

The dependence of heat penetration depth (100 eV isotherm) in gold on laser intensity is shown in figure 3. Also shown in this figure is the result expected from a self-regulating model[9] which does not include radiation transport. It is seen that the laser intensity required for penetration of the high temperature ablation region through a given gold thickness is much larger than that expected from the self-regulating model. On the other hand, examination of ion current signals for gold-coated target at laser intensity well below the burn-through laser intensity showed the existence of a low temperature plastic component, indicating the heating of plastic substrate ahead of the hot plasma ablation of gold overlayer.

The above observations are supported from the X-ray diode measurements of radiation energy in the range ~ 100 eV–2 keV (figure 4). It is seen from this figure that the X-ray yield for the layered targets is smaller than that for the thick gold case even for laser intensities well below the corresponding threshold values for the penetration of 100 eV isotherm. This would indicate the occurrence of significant

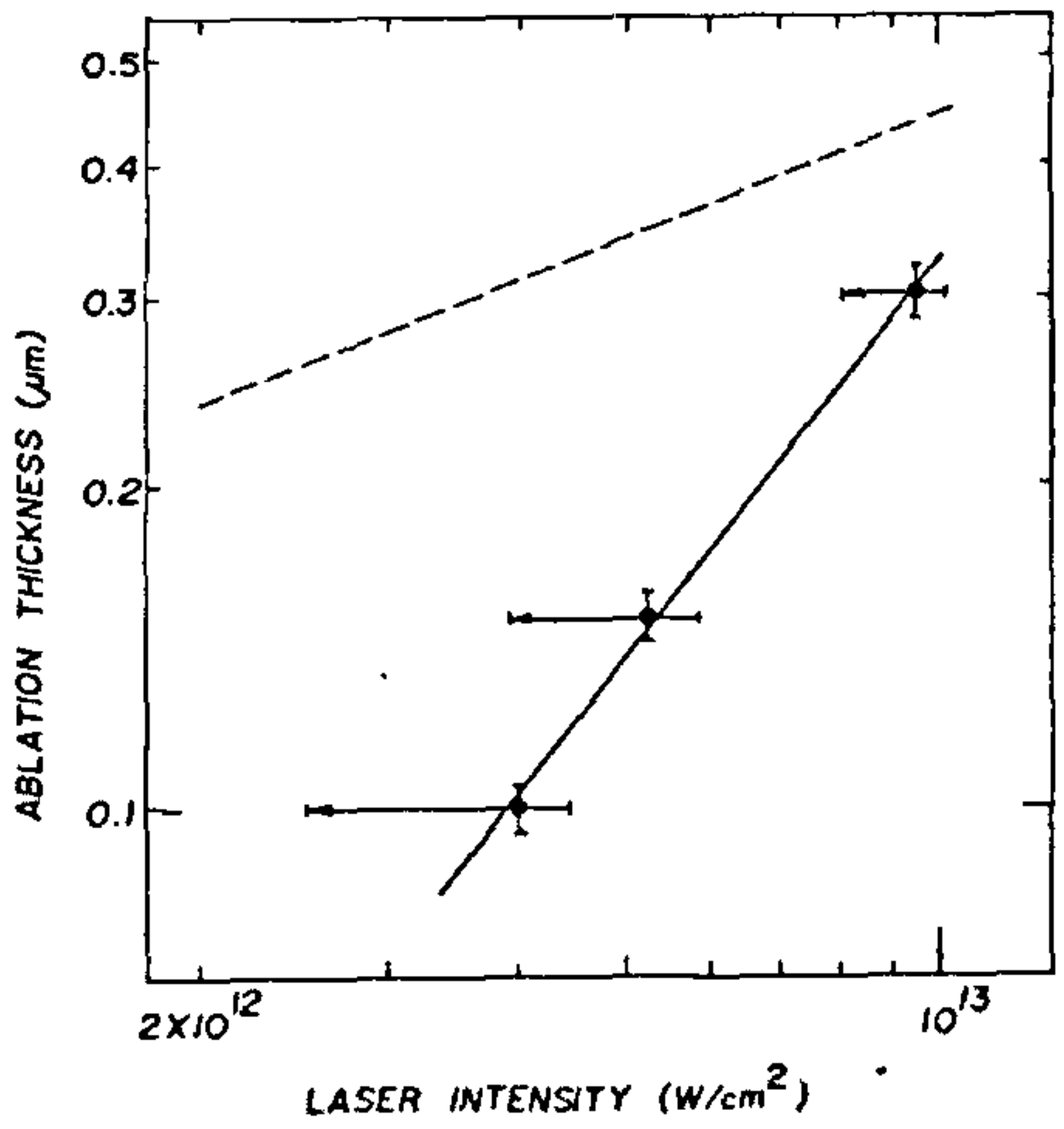

Figure 3. Dependence of penetration depth of the 100 eV isotherm on laser intensity for the gold plasma. The dotted line is the result expected from the self-regulating model.

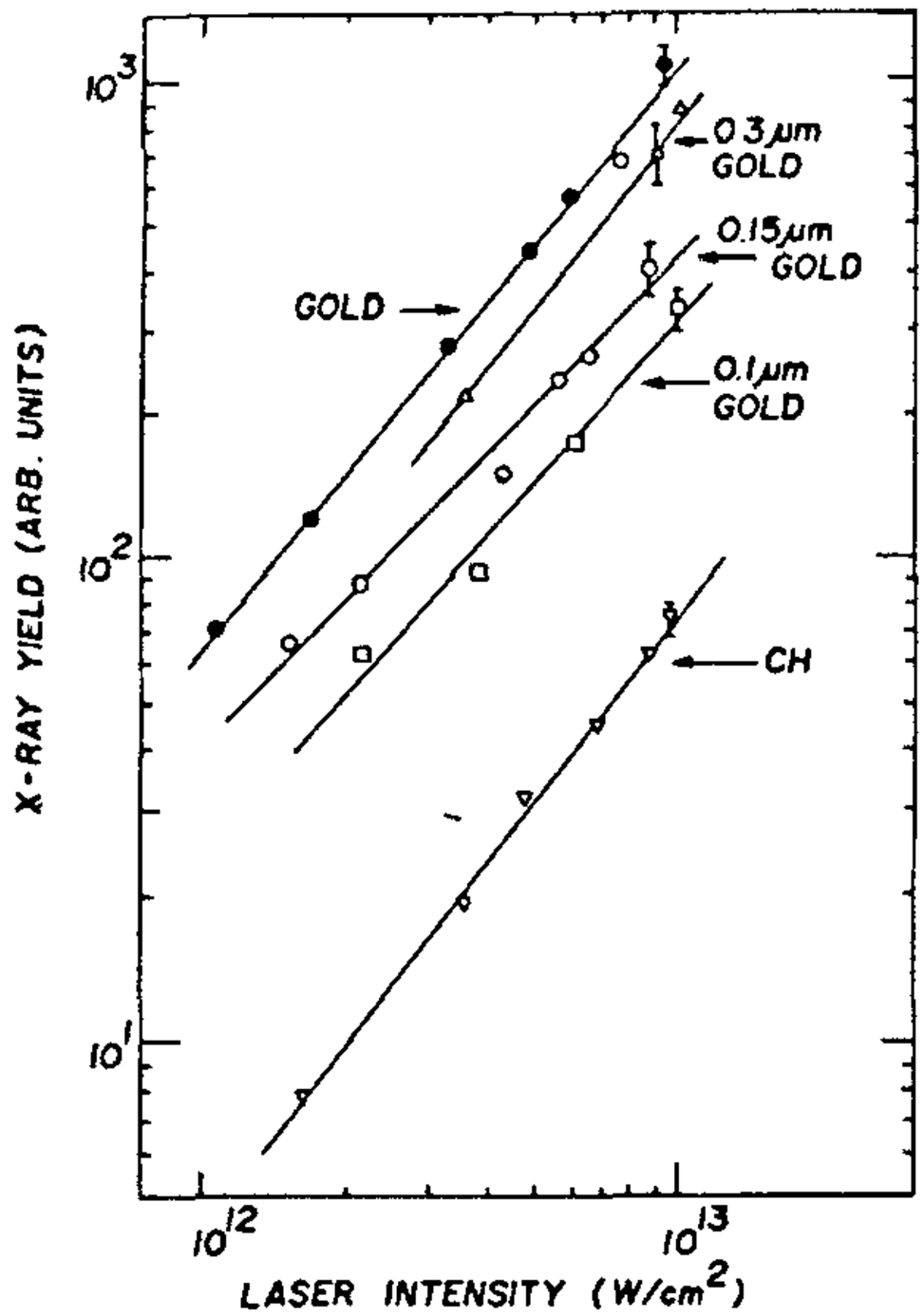

Figure 4. Variation of integrated X-ray diode signal as a function of laser intensity for plastic ▽, gold ●, 0.1 μm, 0.15 μm and 0.3 μm gold-coated targets (□, ○, △) respectively.

energy transport to the low-Z plastic in advance of the 100 eV isotherm. From the relative X-ray yields for targets with different gold layer thicknesses, an *e*-folding penetration depth of 0.3 μm is estimated for this inward propagating energy.

The FWHM duration of keV X-ray emission observed on a X-ray streak camera for thick gold target as well as gold-coated targets was considerably smaller than the FWHM of laser pulse (τ_l). The FWHM of keV X-ray emission for thick gold, 0.3 μm gold-coated target and 0.15 μm gold-coated target was 0.44 ± 0.04, 0.38 ± 0.06 and 0.31 ± 0.04 times τ_l respectively. The smaller duration of keV X-ray emission can be attributed to the cooling of the hot coronal region due to radiation loss into vacuum and inward radiation energy propagation into the plastic substrate. On the other hand, the FWHM duration of sub-keV emission for all targets was longer than that for the laser pulse. For the thick gold target, it was 1.4 τ_l at a laser intensity of 5×10^{12} W/cm^2 and 1.9 τ_l at a laser intensity of 10^{13} W/cm^2.

In view of various observations, the energy penetration to the plastic can be attributed to radiation propagating through the gold overlayer plasma. The high-Z plasma essentially consists of two regions[8]: a high temperature low density coronal region where electron thermal conduction dominates and, further inside, a low temperature, high density optically thick region in which radiation transport dominates. The estimated penetration depth for the radiation transport region of ~ 0.3 μm is in reasonable agreement with the Rosseland mean free path for the approximate conditions of the radiation transport region[8].

The two-region model of high-Z plasma is also consistent with observations of angular distribution and temporal behaviour of the sub-keV X-ray emission. The ratio of X-ray diode signals observed in the direction of 35° and 70° w.r.t. the target normal are 1.02 ± 0.05 for 0.1 μm gold-coated target, 1.11 ± 0.06 for 0.15 μm gold-coated target, 1.21 ± 0.06 for 0.3 μm gold-coated target and 1.28 ± 0.07 for thick gold target. For all the targets the distribution is more isotropic than a $\cos\theta$ distribution for which this ratio is 2.39. It is further noted that for thin gold-coated target, the distribution is nearly isotropic and the departure from isotropy increases with the gold overlayer thickness.

Whereas a $\cos\theta$ distribution is expected for emission from an optically thick plasma with a disc-like surface, an isotropic emission should occur from either an optically thin plasma region or a plasma with a spherical geometry, X-ray emission from the optically thick region (with essentially 1-D flow) is expected to follow a $\cos\theta$ distribution but that from the hot coronal region will be more isotropic. The latter is expected to dominate because the plasma is optically thin in coronal region and because spherical flow is established in the outer region for small focal spot irradiation. The relatively isotropic distribution observed for thick gold indicates the important role of the coronal region in X-ray emission. The

nearly isotropic distribution for thin gold layer coated targets is explained because in this case the inner optically thick region is of CH which is a poor X-ray emitter.

e) *X-ray energy conversion*

X-ray conversion efficiency for $h\nu \geq 100$ eV was measured for targets with different atomic number. X-ray yield was measured using X-ray diodes[15] filtered with 1 μm formvar filters and a X-ray foil calorimeter[16]. The spectral response of X-ray diodes with aluminium cathode and formvar filter is not a flat function[17]. The response can however be approximated as reasonably flat in two distinct regions of 100 eV to 280 eV and 380 eV to 1100 eV. The contribution of the lower energy band was separately measured by using an X-ray diode in conjunction with a high energy cut-off Al_2O_3 mirror.

The dependence of X-ray conversion efficiency on target-Z measured at a laser intensity of 5×10^{12} W/cm^2 is shown in figure 5. The conversion efficiency for aluminium and gold targets is $12 \pm 2\%$ and $36 \pm 6\%$ respectively assuming a cos θ distribution. For aluminium and gold targets the angular dependence on average was observed to fit $(\cos\theta)^{0.76}$ and $(\cos\theta)^{0.33}$ respectively. When these angular distributions are considered, the total X-ray conversion efficiency for aluminium and gold at 5×10^{12} W/cm^2 becomes $13 \pm 2\%$ and $53 \pm 9\%$ respectively. These X-ray conversion estimates are in good agreement with the results obtained from an X-ray foil calorimeter[16].

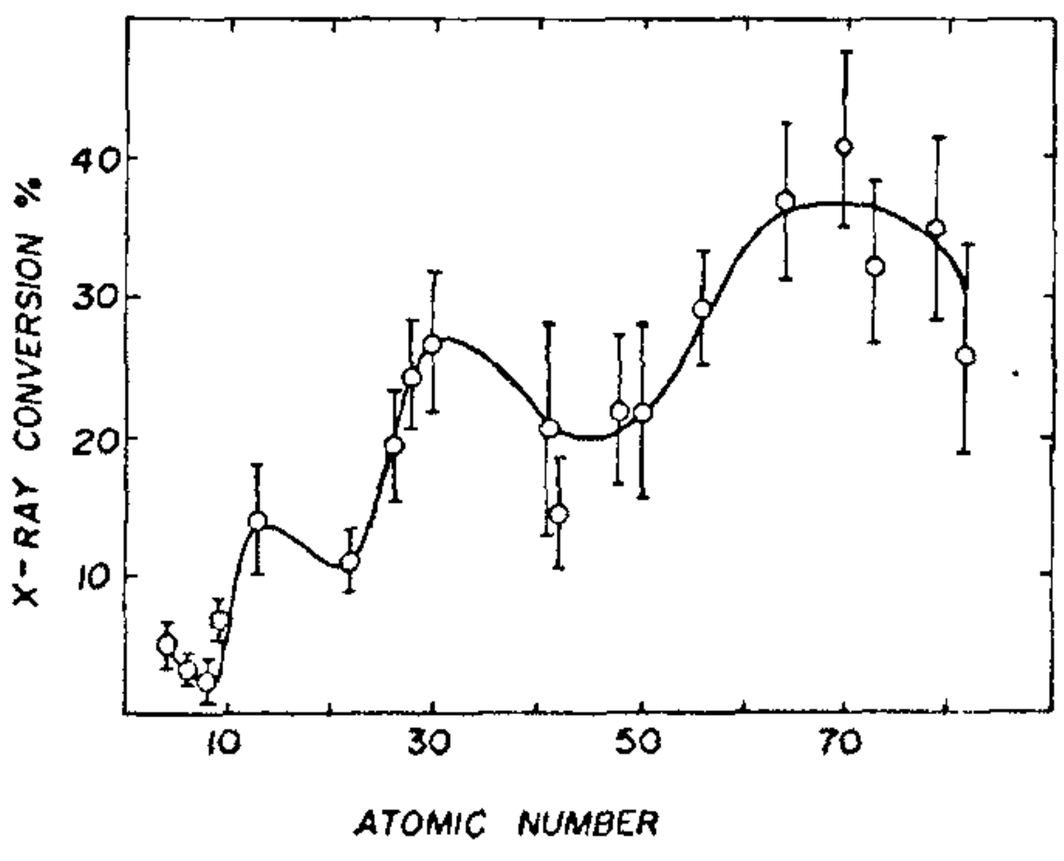

Figure 5. Total X-ray energy conversion as a function of target atomic number at a laser intensity of 5×10^{12} W/cm^2.

CONCLUSIONS

Study of plasma ablation using a KrF laser in the intensity range of 10^{11}–2×10^{13} W/cm^2 has shown high laser energy absorption and an electron temperature scaling consistent with the predictions of a self-regulating model based on the inverse bremsstrahlung-dominated absorption and uninhibited electron thermal conductivity for aluminium plasma. No hot electron component was observed. Mass ablation rate and ablation pressure also show good agreement with the model predictions. For high-Z plasmas, ablation thickness and electron temperature are much smaller than the predictions of self-regulating model without considering radiation effects. Both the radiation loss and the radiation-induced energy transport play an important role in the high-Z laser-plasma interaction. Back reflectivity from the plasma is dominated by specular reflection and the small level of SBS observed is consistent with convective growth of the instability. X-ray yield showed significant modulations with target atomic number. High X-ray energy conversion of $53 \pm 9\%$ is obtained from gold targets at a laser intensity of 5×10^{12} W/cm^2.

ACKNOWLEDGEMENTS

The authors acknowledge the expert technical assistance of B. Harwood, K. Houston and A. Haromy throughout the course of these experiments. This research was supported by the Natural Science and Engineering Research Council of Canada.

29 August 1987

1. Mead, W. C. *et al.*, *Phys. Fluids*, 1984, **27**, 1301.
2. Key, M. H., Toner, W. T., Goldsack, T. J., Kilkenny, J. D., Veats, S. A., Cunningham, P. F. and Lewis, C. L. S., *Phys. Fluids*, 1983, **26**, 2011.
3. Offenberger, A. A., Fedosejevs, R., Mcken, D. C. D., Tomov, I. V., Gupta P. D. and Marchard, R., *Short pulse krypton fluoride laser system using beam multiplexing and stimulated Raman/Brillouin scattering*, Paper presented at CLEO 87, IQEC'87 April 27-May 1, 1987, Baltimore, U.S.A.
4. Mcken, D. C. D., Fedosejevs, R., Arnfield, M., Tomov, I. V., Domier, C. and Offenberger, A. A., *Rev. Sci. Instrum.*, 1983, **54**, 845.
5. Murray, J. R., Goldhar, J., Eimerl, D. and Szoke, A., *IEEE J. Quant. Electron.*, 1979, **QE-15**, 342.
6. Fedosejevs, R. and Offenberger, A. A., *IEEE J. Quant. Electron.*, 1985, **QE-21**, 1558.
7. Gupta, P. D., Popil, R., Fedosejevs, R., Offenberger, A. A., Salzmann, D. and Capjack, C. E., *Appl. Phys. Lett.*, 1986, **48**, 103.
8. Gupta, P. D., Tsui, Y. Y., Popil, R., Fedosejevs, R. and Offenberger, A. A., *Phys. Rev.*, 1986, **A34**, 4103.
9. Mora, P., *Phys. Fluids*, 1982, **25**, 1051.
10. Offenberger, A. A., Fedosejevs, R., Gupta, P. D., Popil, R. and Tsui, Y. Y., *Laser Particle Beams*, 1986, **4**, 329.
11. Gupta, P. D., Tsui, Y. Y., Popil, R., Fedosejevs, R. and Offenberger, A. A., *Phys. Fluids*, 1987, **30**, 179.
12. Gupta, P. D., Tsui, Y. Y., Popil, R., Fedosejes, R. and Offenberger, A. A., *Phys. Rev.*, 1986, **A33**, 3531.
13. Gupta, P. D. and Kumbhare, S. R., *J. Appl. Phys.* 1984, **55**, 120.
14. Gupta, P. D., Tsui, Y. Y., Popil, R., Fedosejevs, R. and Offenberger, A. A., *Optics Commun.*, 1987, **63**, 165.
15. Popil, R., Gupta, P. D., Fedosejevs, R. and Offenberger, A. A., *Phys. Rev.*, 1987, **A35**, 3874.
16. Fedosejevs, R., Tsui, Y. Y., Popil, R., Gupta, P. D., Baker, J. and Offenberger, A. A., *J. Phys.*, 1987 (to be published).
17. Day, R. H., Lee, P., Saloman, E. B. and Nagel, D. J., *J. Appl. Phys.*, 1981, **52**, 6965.

NEWS

US$ 13 MILLION FOR AIDS PREVENTION IN FOUR AFRICAN COUNTRIES

The Special Programme on AIDS of the World Health Organization (WHO) announced that over US$ 13 million has been raised for AIDS prevention and control activities in the coming year for four African countries.

The meetings held in Ethiopia (3–4 August), Kenya (30–31 July), Rwanda (27–28 July) and Tanzania (23–24 July) were attended by representatives of over 25 countries and international agencies. Each meeting was organized by the Ministry of Health concerned and by WHO, following several months of collaboration leading to official endorsement of a comprehensive five-year national AIDS plan.

Since the establishment of the Special Programme on AIDS on 1 February 1987, over 80 countries have requested collaboration. Assessment visits have been made to 44 countries and 37 short-term (6–12 month) plans have been prepared. Comprehensive five-year plans have been officially approved by 13 countries and another seven are in preparation. Over 240 consultant missions have been conducted. By the end of 1987, WHO will be collaborating in the development and strengthening of national AIDS programmes in all countries from every region of the world which have requested support, including virtually all countries of sub-Saharan Africa. (**World Health Organization*, Media Service, 1211, Geneva 27, Switzerland).